

1971

Angular and Energy Distribution of Cross Sections for Electron Production by 50-300-keV-Proton Impacts on N₂, O₂, Ne, and Ar

J. B. Crooks

University of Nebraska - Lincoln

M. Eugene Rudd

University of Nebraska - Lincoln, erudd@unl.edu

Follow this and additional works at: <http://digitalcommons.unl.edu/physicsrudd>



Part of the [Physics Commons](#)

Crooks, J. B. and Rudd, M. Eugene, "Angular and Energy Distribution of Cross Sections for Electron Production by 50-300-keV-Proton Impacts on N₂, O₂, Ne, and Ar" (1971). *M. Eugene Rudd Publications*. 55.
<http://digitalcommons.unl.edu/physicsrudd/55>

This Article is brought to you for free and open access by the Research Papers in Physics and Astronomy at DigitalCommons@University of Nebraska - Lincoln. It has been accepted for inclusion in M. Eugene Rudd Publications by an authorized administrator of DigitalCommons@University of Nebraska - Lincoln.

Angular and Energy Distribution of Cross Sections for Electron Production by 50-300-keV-Proton Impacts on N₂, O₂, Ne, and Ar

J. B. Crooks and M. E. Rudd

Behlen Laboratory of Physics, University of Nebraska, Lincoln, Nebraska 68508

Received 12 November 1970

Cross sections differential in angle and ejection energy for electron production by proton impact on nitrogen, oxygen, neon, and argon have been measured using electrostatic analysis and counting of individual electrons. The range of proton energies was 50-300 keV, the angles ranged from 10° to 160°, and the electron energies were measured from 1.5 to 1057 eV. Integrations over angle and/or electron energy yielded singly differential and total electron production cross sections. Our total cross sections for oxygen fall halfway between previous data of deHeer *et al.* and Hooper *et al.*, but our argon cross sections agree better with deHeer *et al.* Cross sections for electron ejection in the backward hemisphere are much greater for these multishell targets than for hydrogen and helium. The momentum-energy conservation hump which was prominent in hydrogen is less conspicuous for these gases.

Published in *Physical Review A* 3, 1628 - 1634 (1971)

©1971 The American Physical Society. Used by permission.

URL: <http://link.aps.org/doi/10.1103/PhysRevA.3.1628>

DOI: 10.1103/PhysRevA.3.1628

PHYSICAL REVIEW A ₁

VOLUME 3, NUMBER 5

MAY 1971

Angular and Energy Distribution of Cross Sections for Electron Production by 50-300-keV-Proton Impacts on N₂, O₂, Ne, and Ar[†]

J. B. Crooks and M. E. Rudd

Behlen Laboratory of Physics, University of Nebraska, Lincoln, Nebraska 68508

(Received 12 November 1970)

Cross sections differential in angle and ejection energy for electron production by proton impact on nitrogen, oxygen, neon, and argon have been measured using electrostatic analysis and counting of individual electrons. The range of proton energies was 50–300 keV, the angles ranged from 10° to 160°, and the electron energies were measured from 1.5 to 1057 eV. Integrations over angle and/or electron energy yielded singly differential and total electron production cross sections. Our total cross sections for oxygen fall halfway between previous data of deHeer *et al.* and Hooper *et al.*, but our argon cross sections agree better with deHeer *et al.* Cross sections for electron ejection in the backward hemisphere are much greater for these multishell targets than for hydrogen and helium. The momentum-energy conservation hump which was prominent in hydrogen is less conspicuous for these gases.

INTRODUCTION

The production of electrons in fast ion-atom and ion-molecule collisions is of basic interest in a number of areas. The energy distribution of electrons from such collisions is useful in understanding stopping power,¹ energy deposition phenomena,² and auroral and upper atmospheric processes.³ The angular distribution is of considerable importance in testing various theoretical descriptions of the ionization process. Some of the theoretical aspects are discussed in the following paper.⁴

Cross sections for electron ejection which are differential in both angle and energy have become available only in the last few years. Kuyatt and Jorgensen⁵ made the first such measurements for protons of 50–100 keV on hydrogen. Rudd and Jorgensen⁶ made measurements on helium from 50 to 150 keV. The energy range was extended for both gases to 300 keV in the work of Rudd, Sautter, and Bailey.⁷ This enters the region where Born-approximation calculations yield accurate results for total ionization cross sections, but it was shown that the angular distributions were still off by large factors. Cacak and Jorgensen⁸ recently studied Ne⁺-Ne and Ar⁺-Ar collisions from 50 to 300 keV. Torburen⁹ recently measured doubly differential cross sections

for electrons from H⁺-N₂ collisions from 300 to 1700 keV.

In the present work, we have measured angular and energy distributions of electrons from N₂, O₂, Ne, and Ar bombarded by protons from 50 to 300 keV. Comparison of these data with those on hydrogen and helium is made to determine the effect of inner shells on the ionization process. The data on atmospheric gases should be useful in determining the interaction of the protons in the solar wind with the upper atmosphere. Also since oxygen and nitrogen are important constituents of protoplasm, these results can be applied to the problem of energy deposition in cells and tissues.

EXPERIMENTAL METHOD

The apparatus used in this experiment is the same as that used by Rudd and Jorgensen⁶ and modified in the work of Cacak and Jorgensen.⁸ A collimated, magnetically analyzed proton beam entered a chamber containing the target gas at pressures of about 4×10^{-4} Torr. The beam was collected in a shielded, positively biased Faraday cup and integrated. Electrons from a short length of the beam went to a 127° electrostatic analyzer placed at any of eight angles from 10° to 160° from the beam. Before entering the analyzer they were accelerated by

15 V. The detector was a 14-stage Cu-Be electron multiplier (Dumont SPM-03-201) operated in the pulse-counting mode. The multiplier was operated at 4255 V total voltage, with the first dynode kept at 300 V. The resolution full width at half-maximum (FWHM) of the analyzer was 5.7% and the range of angles accepted by the electron collimator was $\pm 1.45^\circ$. The effective solid angle for detection as seen from the target was 5.56×10^{-4} sr. The modifications of the apparatus since the original description⁶ were the following. (i) The pumping of the analyzer and detector regions was improved. The base pressure with no target gas in the chamber was 8×10^{-7} Torr. This rose to about 4×10^{-5} Torr when target gas was admitted. (ii) The Faraday cup was made deeper for better collection and secondary suppression. (iii) Field-straightener electrodes were added to the cylindrical analyzer to minimize fringing fields. (iv) A system of small movable apertures was placed before the analyzer to be used with the beam from an electron gun to determine the efficiency of the detector.

Magnetic fields along the electron path were annulled to within a few milligauss by three mutually perpendicular sets of Helmholtz coil pairs. The target gas pressure was read with a Baratron capacitance manometer. A calculated correction of 12% was applied to compensate for the difference between the pressure at the manometer and at the scattering center due to the effects of gas flow and thermal transpiration between the chamber and the manometer head.

Absorption of electrons between the target and detector was accounted for using data of Normand,¹⁰ Brüche,¹¹ and Golden and Bandel¹² on electron scattering. The efficiency of the detector was determined to be 0.81 ± 0.06 in earlier work.⁸ The same multiplier was used in this experiment but the efficiency has since decreased to 0.73. This was determined by remeasuring cross sections in helium which had been measured at the time of the earlier efficiency determination.

The scaler counting electrons was automatically stopped after a preset number of beam protons (between 1 and 20 μC) was collected at a given analyzer setting. A run through all electron energies was followed in each case by a background run with the gas supply shut off. A subtraction was made both for the residual electron count and the residual gas pressure. After runs were made at all desired combinations of proton energy and type of target gas, helium was admitted to the chamber, the analyzer moved to a port at a different angle, and after pumpdown, measurements at the new angle proceeded. Reruns were later made at some combinations of angle, gas, and beam energy which generally yielded cross sections within 10% of values taken earlier.

Cross sections which were differential in angle only, in energy only, or total cross sections for electron production, were obtained by integration of the doubly differential cross sections as in the earlier work.⁷ Integrations over angle were done by fitting a series of five spherical harmonics to the data, weighting the measurements according to $\sin\theta$. The required integral was then obtained directly from the coefficient of the first spherical harmonic. Integrations over ejected electron energy are difficult to make accurately because an appreciable fraction of the area under the curve is at low-electron energies where, as discussed later, the results are unreliable. The following procedure was used. The low-energy regions of several runs were plotted. These generally have a well-defined smooth region above a certain energy. Using this, the graph was extrapolated to zero energy. The area between the extrapolated and measured curves was measured with a planimeter and found to be generally about 6% of the entire area. A 6% correction was then applied to all cross sections integrated over energy.

The proton beam was partially neutralized by capture between the scattering center and the Faraday cup. Using the data of Ref. 13 this effect was calculated for each combination of beam energy and gas type and a correction was made. The largest value of this correction was 7% for 50-keV protons in argon and was generally much smaller.

DISCUSSION OF ERRORS

Considering the accuracy of the capacitance manometer and the uncertainty in the correction made on the pressure reading, we estimate the uncertainty in the pressure to be 12%. The uncertainty in the value for detector efficiency is 10%. These were the two major sources of error in the experiment over nearly all of the ranges of parameters. Errors in the geometrical factors, ion-beam integration, calculation of the electron transmission, and effective analyzer width were all of the order of 1 or 2%. The doubly differential cross sections thus have an uncertainty of 16%. The uncertainty due to counting statistics becomes appreciable only when the cross section is smaller than about 10^{-26} $\text{m}^2/\text{eV sr}$, and becomes dominant below about 10^{-28} $\text{m}^2/\text{eV sr}$. Typical combined uncertainties are shown for three cross-section values on Fig. 1. At low electron energies, the effect of residual magnetic fields and electric fields becomes important. Unfortunately, it is difficult to estimate these fields and their effects, but the day-to-day reproducibility of our data becomes progressively worse below about 12 eV, and the data are completely unreliable below 3 or 4 eV. Also, our agreement with other work and with theory is poor in this region.

Integration of cross sections over angle or energy involves additional errors but also some averaging.

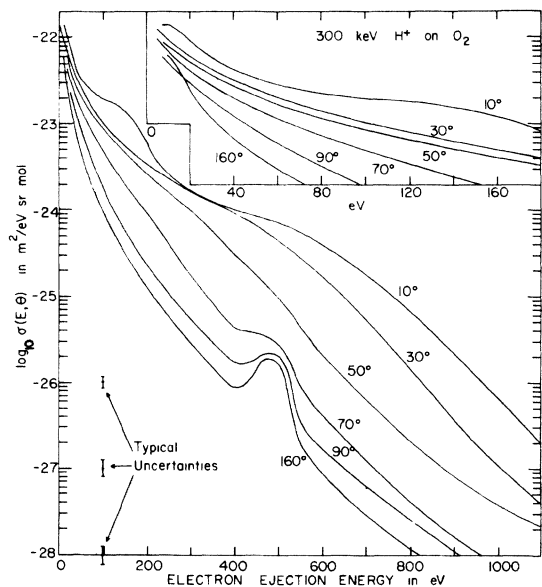


FIG. 1. Doubly differential cross sections for ejection of electrons from oxygen gas by 300-keV-proton impact. Inset shows low-energy region with expanded energy scale. Analyzer resolution was 5.7%.

With the correction for the depression of cross-section values at low energies mentioned previously, it is unlikely that there is more than about 5% error introduced by the integration. A similar error is involved in the angular integration. The total cross

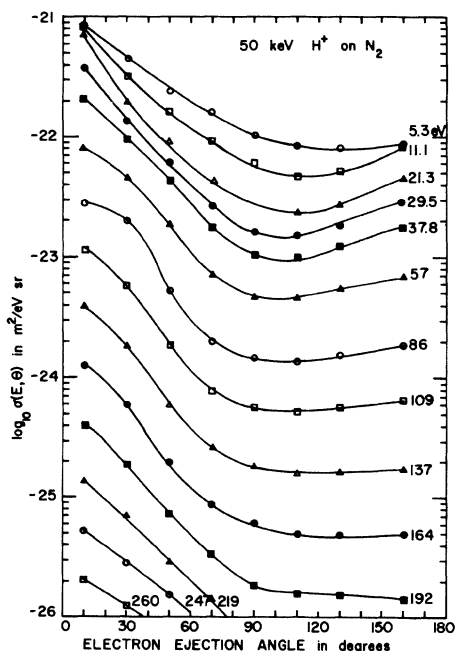


FIG. 2. Angular distribution of electrons of various energies from 50-keV-proton impacts on nitrogen gas.

sections for production of electrons are then uncertain by about 17%.

EXPERIMENTAL RESULTS

Since this experiment involves such a large amount of data (over 8000 separate cross sections were measured), only representative samples will be presented.¹⁴

The doubly differential data can be given as energy distributions with angle as a parameter as in Fig. 1 and as angular distributions with energy of the electron as a parameter as in Fig. 2. The cross section generally falls off with increasing electron energy but has a few features of interest. In the curves at the large angles the Auger peak is prominent (at about 500 eV for oxygen) but is harder to distinguish in the forward directions where the continuum cross section is larger. Auger emission, in those few cases where its angular distribution has been experimentally measured,^{8,15} appears to be essentially isotropic. The data here tend to support this finding.

In the graph for 10° in Fig. 1, there are two broad humps which have been seen previously.^{6,7} The higher energy hump (at about 600 eV in Fig. 1), as noted by Toburen,⁹ is at the energy predicted by conservation of energy and momentum applied to a collision between a proton and a free electron. Furthermore, the shape of the hump is described, though somewhat inaccurately, in the Born-approx-

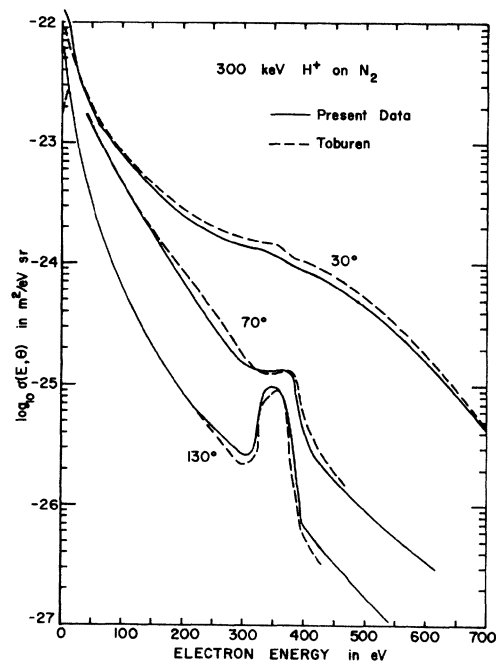


FIG. 3. Comparison of doubly differential cross sections with data of Toburen (see Ref. 9) for three angles of ejection.

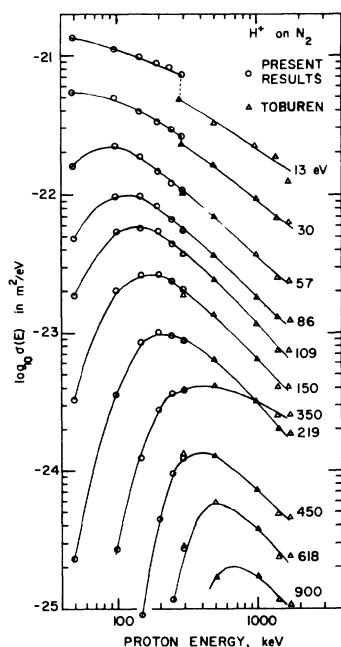


FIG. 4. Cross sections for ejection of electrons of various energies (integrated over all angles) from proton impacts on nitrogen gas. Data of Toburen are from Ref. 9. Curve at 350 keV is in the Auger region.

imation calculation of cross sections.⁷ The other hump (at about 150 eV in Fig. 1) is a result of the influence of the beam particle after the collision. Electrons are carried along in the forward direction before ejection, a process which may be called charge transfer into continuum states. This effect has been treated formally by Macek¹⁶ and by Salin.¹⁷ This hump occurs at the velocity of ejection equal to the proton velocity, and is strongly peaked about the forward direction. This is why it is seen only in the 10° curve.

Figure 2 gives the angular distribution of various energy electrons ejected in 50-keV collisions of protons and nitrogen molecules. The cross sections all fall off from 0° to 90° and thereafter are constant or even rise slightly in some cases.

A comparison of our N₂ data at 300 keV is possible with the work of Toburen,⁹ and is shown in Fig. 3 for three different angles. Above 15 eV, the greatest discrepancy is 20%, well within the combined uncertainties of the two measurements. Below this energy, electric and magnetic fields strongly affect the results and are difficult to control. Furthermore, secondary electrons from surfaces are more numerous at these low energies. Considering these factors, the agreement is considered to be very good. We can also compare our 100-keV data for argon with earlier work at one angle in our laboratory (using a different collision chamber and analyzer) by Rudd, Jorgensen, and Volz.¹⁸ Here the

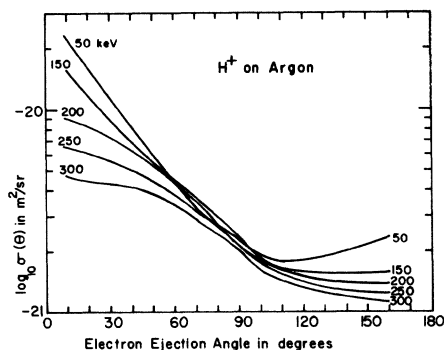


FIG. 5. Cross sections for ejection of electrons of all energies as a function of angle for various proton energies in argon.

discrepancy is less than the smaller uncertainty of the present experiment.

In Fig. 4 our results integrated over all angles are plotted with those of Toburen⁹ vs proton energy. Except at the lowest electron energies the data fit together smoothly. The curves for various ejected electron energies are similar, increasing to a maximum and then falling off somewhat less rapidly. The proton energy at the maximum increases linearly with electron energy. The curve at 350 eV is different from the rest since that energy is at the Auger peak. This cross section is the sum of two parts; one due to electrons in the continuum which come mostly from outer-shell collisions, and the other due to Auger electrons resulting from inner-shell vacancies. At lower proton energies the direct process predominates but as the energy is increased the Auger process becomes more impor-

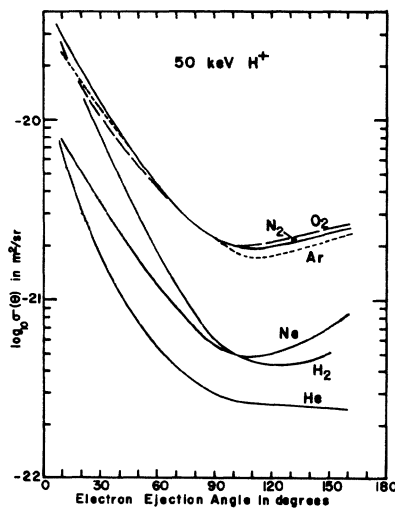


FIG. 6. Cross sections for ejection of electrons of all energies as a function of angle for 50-keV protons bombarding various gases. Hydrogen data are from Ref. 5 and helium data from Ref. 6.

tant. Since inner-shell processes peak at higher energies, the curve is skewed.

Cross sections differential in angle but integrated over all electron energies are shown in Figs. 5 and 6. In Fig. 5, data for one gas Ar are plotted for several impact energies. In Fig. 6, data for various gases are shown at one impact energy, 50 keV. From these graphs it is clear that the lower the bombarding energy the more peaked is the distribution in the forward direction but also more are present in the backward direction. Between 60° and 110° the cross sections are nearly independent of impact energy. He and H_2 have somewhat steeper angular distributions than the other four gases, the latter tending to have similar shapes but with Ne lower in absolute magnitude by about a factor of 4.

Total cross sections for electron production are given in Table I. Figure 7 shows a plot of our O_2 data along with those of deHeer *et al.*¹⁹ and Hooper *et al.*²⁰ The rather large discrepancy between these two previous sets of data makes our results of particular significance. At low proton energies we agree well in slope and absolute value with deHeer and at high energies equally well with Hooper, splitting the difference at 150 keV. Similar results occur in the case of Ne and N_2 but in Ar our high-energy cross sections are about 25% smaller than those of Hooper.

COMPARISON OF CROSS SECTIONS FOR VARIOUS TARGETS

Figure 8 shows, at 300-keV impact energy, a comparison of cross sections for the four gases at the extreme angles 10° and 160° . In addition, earlier data⁷ for H_2 and He at 10° are plotted for comparison. Auger peaks are prominent in the 160° curves but are nearly absent at 10° as discussed before. The Ar Auger peak at 200 eV is due to an L-shell vacancy and has been investigated at higher resolution previously.^{18,21} The other three targets

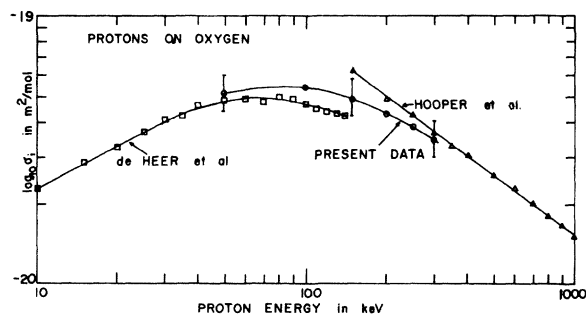


FIG. 7. Total cross sections for electron ejection from oxygen gas by protons vs proton energy. Data of deHeer *et al.* are from Ref. 19 and data of Hooper *et al.* are from Ref. 20.

TABLE I. Total cross sections for electron production by proton impact (units are 10^{-20} m^2).

Proton energy (keV)	Nitrogen	Oxygen	Neon	Argon
50	5.53	5.18	1.51	5.13
100	5.37	5.44	1.69	5.17
150	4.69	4.91	1.71	4.55
200	4.13	4.34	1.57	3.96
250	3.63	3.87	1.47	3.43
300	3.24	3.47	1.36	3.01

show K Auger peaks.

Except for the Auger peaks, the 160° curves for the four gases are similar in shape although at high energies the Ar cross sections are appreciably greater than those of the other targets. Both the H_2 and He 160° curves fall off more rapidly with energy than any of the present four gases.

In the 10° curves the Ar cross sections fall off more steeply at low energies than the other multi-shell targets and almost as rapidly as H_2 and He. Also noteworthy is the fact that the momentum-energy conservation hump (at about 600 eV) which is quite prominent in H_2 is less conspicuous for the other gases and, in fact, is nearly absent in Ne. One might expect that targets with the least tightly bound electrons (such as oxygen) would have the most prominent maxima but this is not always the

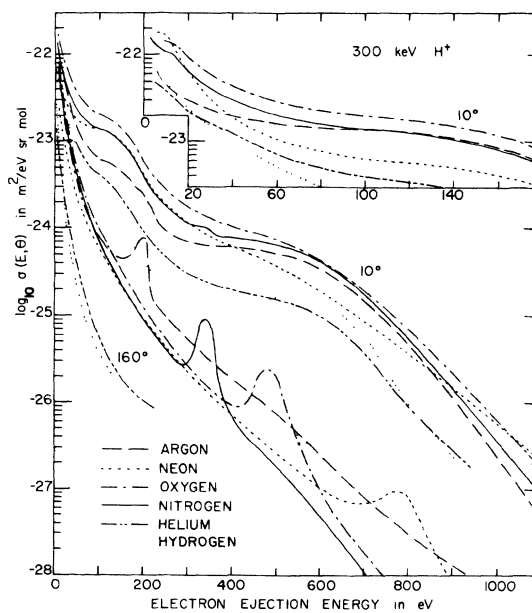


FIG. 8. Doubly differential cross sections for electrons from 300-keV-proton bombardment of six gases. Auger peaks show up in the 160° curves. Data on hydrogen and helium are taken from Ref. 7.

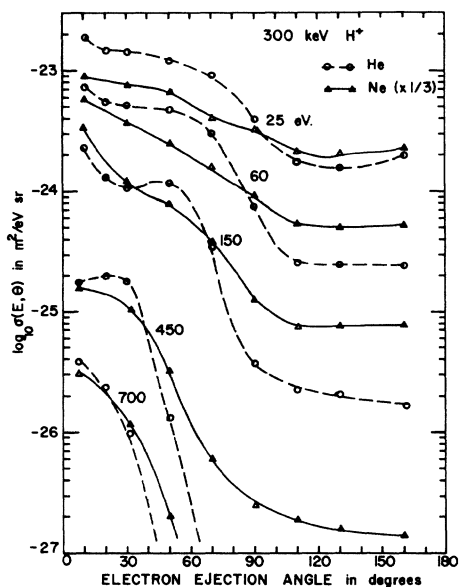


FIG. 9. Comparison of angular distribution of electrons from helium and neon.

case. He with a binding energy of 24.6 eV has a slightly more pronounced hump than O_2 with 12.1 eV binding energy. This could be due either to the presence of inner shells or to the different angular momenta of the outer shells. The same effect is seen in a different way in Fig. 9, where the angular distributions of electrons from He and Ne are compared. The momentum-energy conservation maximum appears at different angles for different electron energies and is especially prominent at about 50° in the 150-eV curves. Ne has a weaker maxi-

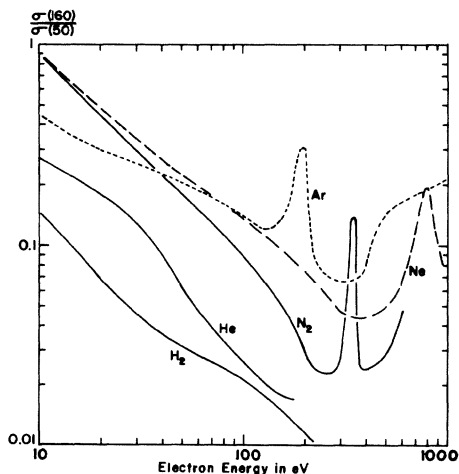


FIG. 10. Ratio of doubly differential cross sections at 160° to that at 50° vs ejected electron energy for five gases. Data on oxygen were omitted for clarity but are similar to those for nitrogen.

mum than He. Both gases here have about the same ionization potential (24.6 and 21.6 eV for He and Ne, respectively), but differ again in the presence of inner shells in one case and also in the angular momentum of the outer shells. With the data available it is not possible to say for sure which effect is more important. This question could be resolved by making calculations of angular distributions of electrons from p states to compare with those for s states already available. Also measurements using targets with inner shells but with outer s electrons (e.g., sodium vapor) would shed light on the question.

Another way in which the ionization of various targets differs is in the relative number of electrons ejected in the backward hemisphere. In Fig. 9, e.g., it is seen that the cross sections above 90° are relatively much smaller for He than for Ne. To put this on a more quantitative basis we have calculated the ratio of the doubly differential cross sections at 160° to that at 50° as a function of electron energy for the various targets under 300-keV-proton bombardment (see Fig. 10). This measure of the back-to-front ratio is smallest at all energies for H_2 , somewhat larger for He, and still larger for the remaining gases. Again, it is not possible to determine from these data whether the differences are due to the effect of the inner shells or to the angular momentum of the outer shell. However, it seems reasonable that the larger fields associated with the greater binding energy of helium and the inner

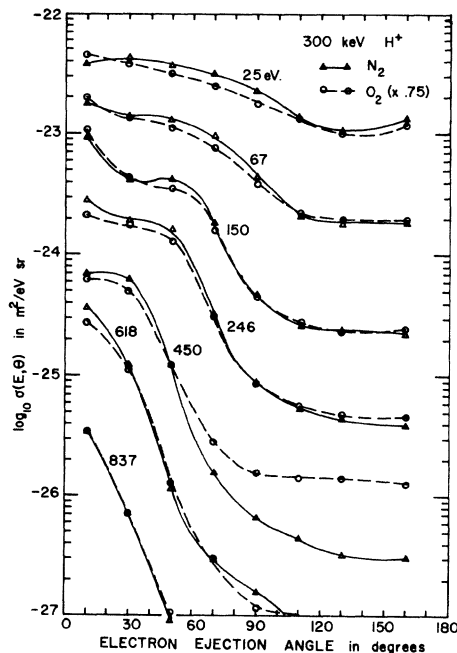


FIG. 11. Comparison of angular distribution of electrons for nitrogen and oxygen.

shells of the other targets would cause greater curvature of the electron paths after ejection and that this could largely account for the greater number of electrons in the backward hemisphere in comparison to hydrogen.

From the scaling equation presented earlier⁷ it can be deduced that most of the cross section is attributable to ionization of the least tightly bound electrons. Also the equation says that for atoms with the same ionization potential the cross section is proportional to the number of electrons. To check this we may compare cross sections for N_2 and O_2 . These have nearly the same ionization potentials, the same inner shells, both have $2p$ outer

electrons, and both are diatomic molecules. They differ, then, primarily in the number of outer subshell electrons, the ratio being 3 to 4. In Fig. 11, O_2 data have been multiplied by 0.75 and compared with N_2 . The cross sections agree in magnitude and shape to within 20% over nearly the entire range of angles and electron energies. A slightly better fit could have been obtained if the O_2 cross sections had been multiplied by 0.8 or 0.85. If we take account of the entire $n=2$ shell the ratio of numbers of electrons is 0.83. The disagreement at 452 eV in the graph is due to oxygen Auger electrons which enhance the cross section at large angles for that energy.

[†]Work supported by the National Science Foundation.

¹J. Cuevas, M. Garcia-Munoz, P. Torres, and S. K. Allison, *Phys. Rev.* **135**, A335 (1964).

²E. J. Kobetich and Robert Katz, *Phys. Rev.* **170**, 391 (1970).

³D. R. Bates, M. R. C. McDowell, and A. Omholt, *J. Atmospheric Terrest. Phys.* **10**, 51 (1957).

⁴M. E. Rudd, D. Gregoire, and J. B. Crooks, following paper, *Phys. Rev. A* **3**, xxx (1971).

⁵C. E. Kuyatt and T. Jorgensen, Jr., *Phys. Rev.* **130**, 1444 (1963).

⁶M. Eugene Rudd and T. Jorgensen, Jr., *Phys. Rev.* **131**, 666 (1963).

⁷M. E. Rudd, C. A. Sautter, and C. L. Bailey, *Phys. Rev.* **151**, 20 (1966).

⁸R. K. Cacak and T. Jorgensen, Jr., *Phys. Rev. A* **2**, 1322 (1970).

⁹L. H. Toburen, *Phys. Rev. A* **3**, 216 (1971).

¹⁰C. E. Normand, *Phys. Rev.* **35**, 1217 (1930).

¹¹E. Brüche, *Ann. Physik* **83**, 1065 (1927).

¹²D. E. Golden and H. W. Bandel, *Phys. Rev.* **138**,

A14 (1965); **149**, 58 (1966).

¹³C. F. Barnett and J. H. K. Reynolds, *Phys. Rev.* **109**, 355 (1958); P. M. Stier and C. F. Barnett, *ibid.* **103**, 896 (1956).

¹⁴A complete set of tabulated cross sections may be obtained on request from the second author. Also available from him are tables of data from the work of Rudd *et al.* (Ref. 7) and Cacak and Jorgensen (Ref. 8).

¹⁵D. J. Volz and M. E. Rudd, *Phys. Rev. A* **2**, 1395 (1970).

¹⁶J. Macek, *Phys. Rev. A* **1**, 235 (1970).

¹⁷A. Salin, *J. Phys. B* **2**, 631 (1969).

¹⁸M. E. Rudd, T. Jorgensen, Jr., and D. J. Volz, *Phys. Rev.* **151**, 28 (1966).

¹⁹F. J. deHeer, J. Schutten, and M. Moustafa, *Physica* **32**, 1766 (1966).

²⁰J. W. Hooper, D. S. Harmer, D. W. Martin, and E. W. McDaniel, *Phys. Rev.* **125**, 2000 (1962).

²¹W. Mehlhorn and D. Stalherm, *Z. Physik* **217**, 294 (1968).